Two-Channel Conductivity and Carrier Crossover in $Co_xNi_{1-x}(pc)I$, Alloys of the Molecular Conductors (Phthalocyaninato)nickel Iodide and (Phthalocyaninato)cobalt Iodide

Kwangkyoung Liou,[†] Claus S. Jacobsen,[‡] and Brian M. Hoffman*,[†]

Contribution from the Department of Chemistry, Northwestern University, Evanston, Illinois 60208, and Physics Laboratory III, Technical University of Denmark, DK-2800 Lyngby, Denmark. *Received September 22, 1988*

Abstract: "Alloys" of the isostructural porphyrinic molecular conductors (phthalocyaninato)cobalt iodide, Co(pc)I, and (phthalocyaninato)nickel iodide, Ni(pc)I, of composition $Co_xNi_{1-x}(pc)I$, $x = 0.02, 0.10, 0.15, 0.20, 0.33, 0.50, 0.75, 0.90$, and 0.95, have been prepared and shown to be homogeneous solid solutions by EPR and energy-dispersive X-ray microprobe analysis. The high ($\sigma_{RT} \sim 500\ \Omega^{-1}\ cm^{-1}$) metallic conductivity of Ni(pc)I ($x = 0$) is associated with holes (positive thermopower) created by partial oxidation from the valence π-band of the pc macrocycle, whereas the lower ($\sigma_{RT} \sim 50\ \Omega^{-1}\ cm^{-1}$) nonmetallic conductivity of Co(pc)I ($x = 1$) is associated with electron carriers (negative thermopower) in the partially oxidized d_{z^2} band of the metal-ion spine. For $x \lesssim 0.75$ EPR and static susceptibility measurements show the existence of Co^{2+} ($S = {}^1/_2$) local moments, although collective effects progressively modify both the EPR intensity and Curie constant as x increases. For $0 \leq x \lesssim 0.2$ the thermopower and magnetic data indicate that the band filling on the macrocycle is constant and the cobalt sites retain their Co^{2+} valency, although the room-temperature conductivity falls ~3-fold and a maximum appears in the conductivity between 170 and 260 K. This change is attributed to paramagnetic scattering by the Co^{2+} local moments. With further increase in x the conductivity continues to change smoothly toward the nonmetallic behavior of Co(pc)I. Surprisingly, the thermopower does not smoothly tend toward the large negative values for Co(pc)I but becomes increasingly positive as x is increased from 0.2 to 0.75 and begins to decrease only by $x \sim 0.90$. These results are interpreted to mean that alloys with $0.2 \lesssim x \lesssim 0.75$-0.9 exhibit two independent conduction channels, hole carriers on the pc macrocycles and electron carriers on the metal-ion spine, and that the site of oxidation shifts progressively from the macrocycle to the metal ion as x is increased. Only by $x \sim 0.95$ (and $T \sim 240$ K) does the thermopower become negative, which signifies the crossover point beyond which all charge-transport behavior is determined by the electron carriers on the metal spine rather than the hole carriers on the macrocycle.

In the present study "alloys" between the two porphyrinic molecular conductors[1-4] (phthalocyaninato)cobalt(II) iodide, Co(pc)I,[3] and (phthalocyaninato)nickel(II) iodide, Ni(pc)I,[4] have been prepared and shown to be homogeneous solid solutions. Crystals of the parent materials Co(pc)I ($x = 1$) and Ni(pc)I ($x = 0$) are isostructural with metal-over-metal columnar stacks of partially (one-third) oxidized M(pc) units surrounded by chains of I_3^- counterions. However, charge transport in Co(pc)I is remarkably different from that in Ni(pc)I. The latter has a high room-temperature conductivity and exhibits metallic behavior; namely, it increases upon cooling. The conductivity of Co(pc)I at room temperature is about one-tenth that of Ni(pc)I and is nonmetallic, decreasing continuously on cooling. These differences in charge transport arise because of a difference in the site of partial oxidation.[3] The oxidation in Co(pc) is metal-centered, and Co(pc)I is a metal-spine conductor whose carriers are electrons (negative thermopower) in a less than half-filled band associated with the cobalt d_{z^2} orbitals. In contrast, oxidation of Ni(pc) is ligand centered, and Ni(pc)I is an organic conductor whose carriers are holes (positive thermopower) associated with a band made up of the π-HOMO of the macrocycles.[4]

Alloys[5] of Ni(pc)I and Co(pc)I with the full range of compositions of $Co_xNi_{1-x}(pc)I$ now have been used to investigate the response of the charge-transport and magnetic properties as the percentage of the paramagnetic Co^{2+} ion is increased from $x = 0$ to $x = 1$ and most especially to search for and characterize the crossover as the site of oxidation shifts from macrocycle to metal ion with increasing x. An analogous shift in oxidation site has been reported for individual (isolated) metallomacrocycles.[6]

Experimental Section

Preparation of $Co_xNi_{1-x}(pc)I$. Co(pc) and Ni(pc) were purchased from the Eastman Kodak Co. and doubly sublimed prior to use. Iodine was obtained from the Mallinckrodt Co. and used without further purification. Co(pc) and Ni(pc) were ground together in a mortar and pestle and then cosublimed to form $Co_xNi_{1-x}(pc)$. Single crystals of

Table I. Elemental Analyses of $Co_xNi_{1-x}(pc)I$[a]

at. ratio x	C	H	N	I
0.02	55.04	2.28	15.92	18.78
0.10	54.95	2.22	15.98	18.50
0.15	55.12	2.34	16.07	18.42
0.20	55.45	2.31	16.07	18.26
0.33	55.31	2.22	15.99	18.00
0.50	54.95	2.20	15.69	18.26
0.75	54.97	2.24	15.85	18.14
calc[b]	55.04	2.31	16.04	18.17

[a] Analyses were done by Micro-Tech Laboratory, Inc., Skokie, IL. [b] Because the atomic weights are Co (58.93) and Ni (58.71), the value of x is effectively irrelevant.

[†] Northwestern University.
[‡] Technical University of Denmark.

(1) For a general overview of work on molecular conductors, see: (a) Proceedings of the Internal Conference on the Physics and Chemistry of Low Dimensional Synthetic Metals (ICSM 84) Parts C and D, Conducting Crystals. *Mol. Cryst. Liq. Cryst.* **1985**, *119*, *120*, Pecile, C., Zerbi, G., Bozio, R., Girlando, A., guest Eds. (b) Williams, J. M.; Beno, M. A.; Wang, H. H.; Leung, P. C. W.; Emge, T. J.; Geiser, U.; Carlson, K. D. *Acc. Chem. Res.* **1985**, *18*, 261. (c) Wudl, F. *Acc. Chem. Res.* **1984**, *17*, 227.

(2) For representative discussions of porphyrinic molecular conductors, see: (a) Hoffman, B. M.; Ibers, J. A. *Acc. Chem. Res.* **1983**, *16*, 15-21. (b) Ogawa, M. Y.; Martinsen, J.; Palmer, S. M.; Stanton, J. L.; Tanaka, J.; Greene, R. L.; Hoffman, B. M.; Ibers, J. A. *J. Am. Chem. Soc.* **1987**, *109*, 1115-1121. (c) Yakushi, K.; Sakuda, M.; Hamada, I.; Kuroda, H.; Kawamoto, A.; Tanaka, J.; Sugano, T.; Kinoshita, M. *Synth. Met.* **1987**, *19*, 769-774. (d) Almeida, M.; Kanatzidis, M. G.; Tonge, L. M.; Marks, T. J.; Marcy, H. O.; McCarthy, W. J.; Kannewurf, C. R. *Solid State Commun.* **1987**, *63*, 457-461. (e) Wynne, K. J. *Inorg. Chem.* **1985**, *24*, 1339-1343. (f) Hanack, M. *Mol. Cryst. Liq. Cryst.* **1988**, *160*, 133-137. (g) Mossoyan-Deneux, M.; Benlian, D.; Baldy, A.; Pierrot, M. *Mol. Cryst. Liq. Cryst.* **1988**, *156*, 247-256. (h) Pietro, W. J.; Marks, T. J.; Ratner, M. A. *J. Am. Chem. Soc.* **1985**, *107*, 5387-5391.

(3) Martinsen, J.; Stanton, J. L.; Greene, R. L.; Tanaka, J.; Hoffman, B. M. *J. Am. Chem. Soc.* **1985**, *107*, 6915-6920.

0002-7863/89/1511-6616$01.50/0

Table II. Co_xNi_{1-x}(pc)I: Quantitative EDS Analyses, Room-Temperature Conductivity,[a] and Magnetic Susceptibility Parameters[b]

	fraction x of Co(pc) in reactants								
	0	0.02	0.10	0.15	0.20	0.33	0.50	0.75	1.0
EDS value of x in alloy	0	0.02	0.10	0.14	0.20	0.35	0.47	0.78	1.0
room temp cond[b] Ω^{-1} cm^{-1}	500	500	450	350	200	150	100	60	60
C_{obs} (Curie const), emu/mol × 10^{-2}				4.1	5.4	7.4		3.7	
C_{obs}/C_{calc}				0.45	0.44	0.33		0.07	
θ, K				−0.7	−2.0	−2.4		−2.4	
χ_p, emu/mol × 10^4				2.3	2.7	2.3		3.4	

[a] The values of σ_{RT} are obtained from four-probe (27 Hz) measurements, and each is an average of numerous determinations. Uncertainties in these average values are estimated to be ±15%. [b] Parameters defined in eq 3 and text.

alloys, Co_xNi_{1-x}(pc)I, with x = 0.02, 0.10, 0.15, 0.20, 0.33, 0.50, 0.75, 0.90, and 0.95, were grown by codiffusion of the 1-chloronaphthalene solutions of Co_xNi_{1-x}(pc) and molecular iodine in an H-tube at a relative high temperature (140–160 °C) to eliminate the possibilities of selective transport of the more soluble Ni(pc) units. These crystals are isostructural with the parent materials. Elemental analyses are given in Table I.

Deiodinated samples (Δ-Co_xNi_{1-x}(pc)) were prepared by gentle heating ($T \sim 100$ °C) of the iodinated Co_xNi_{1-x}(pc)I materials under vacuum for several days. The resulting materials have the purplish luster of the cosublimed parent materials in contrast to the gold-greenish luster of the oxidized alloys.

Microprobe Analysis. Microprobe determination of the Co/Ni ratio was performed with the JEOL Superprobe 733 system. Crystals were mounted on the cylindrical copper alloy holder by application of the conductive carbon paint (SPI No. 5006) and were coated with carbon vapor to prevent charge accumulation. Pure Co(pc)I and Ni(pc)I were used as standards for the quantitative analysis of Co Kα, E = 6.93 keV, and Ni Kα, E = 7.46 keV. Quantitative analysis uses a focused beam with diameter of ~10 μm. Compositional homogeneity along an individual crystal was checked by using the focused beam to analyze numerous points on several crystals from each of a number of different batches. The composition mode uses an unfocused beam and gives a qualitative measure for an entire preparation. X-ray emissions characteristic of iodine (L_α = 3.94, L_β = 4.23 keV), were monitored to confirm the complete removal of iodine in the deiodinated samples.

Electron Paramagnetic Resonance Measurement. X-band EPR spectra at ca. 9 GHz were obtained on modified Varian E-4 or E-9 spectrometers. Spectra of deiodinated samples were recorded at room temperature and 77 K. EPR measurements at $5 \lesssim T < 77$ K employed an Air Product Model LTR cryostat system. Powder samples were employed for all experiments because the EPR signals of single crystals were too broad to be detected for both oxidized and deiodinated materials.

Charge-Transport Measurement. Four-probe (27 Hz) conductivity measurements along the crystal axis over the temperature range 100–300 K were done using the ac phase-locked apparatus and techniques described elsewhere.[3,7a] Crystals of typical length of 2–3 mm and width of 0.01–0.02 mm were mounted on silvered graphite fibers by using palladium paint.

Thermoelectric Power. The technique used for measuring thermopower was similar to that described by Chaikin and Kwak.[7b] A slow alternating temperature gradient with a maximum temperature drop of less than 1 K was employed along the needle-shaped samples. The thermopower, S, was measured against that of pure gold, the contact material being Pd paint. All data are corrected for the thermopower of gold.

Magnetic Susceptibility. Static magnetic susceptibilities were measured by using a SHE Corp. Model VTS-10 superconducting quantum-interference device (SQUID) susceptometer. Sample holders were made of high-purity Supersil quartz because signals of metallophthalocyanine iodides are small relative to the background values of the usual Si–Al bucket (ca. $^1/_{20}$). Before a sample was run, the holder background was checked over the full experimental temperature range: calibration of the instrument was routinely done by using Pd powder, the NBS standard.

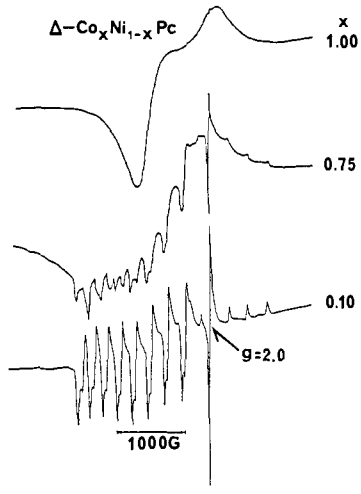

Figure 1. EPR spectra of deiodinated samples, Δ-Co_xNi_{1-x}(pc), x = 100, 0.75, and 0.10.

Variable-temperature measurements were done at 10 kG with approximately 30-mg samples; the field dependence was not studied because the susceptibilities of the parent compounds, Ni(pc)I and Co(pc)I, are invariant over the range of fields, 5–50 kG.

Results

Composition of Co_xNi_{1-x}(pc)I. The following ratios of starting materials of the type Co_xNi_{1-x}(pc) were chosen as representing a broad range of compositions: x = 0.02, 0.10, 0.15, 0.20, 0.33, 0.50, 0.75, 0.90, and 0.95 (by weight). After cosublimation of the above starting mixtures, batches of needlelike crystals with golden-greenish luster identical in form with those of the x = 0 and x = 1 parent conductors were produced by iodine oxidation. Elemental analyses of these materials were reasonably matched to the calculated values for the main elements (C, H, N, I; Table I).

Quantitative microprobe studies were used to determine the metal content of the alloys, Co_xNi_{1-x}(pc)I, as well as their homogeneity on the macroscopic level of the electron beam diameter, ~10 μm. In all cases the measured value of x was in good agreement with the initial mixing ratio of the starting materials (Table II) and was consistent across a single crystal and within a batch of crystals within a relative error less than ± 5%. Measurements in the composition mode also indicated that the samples were homogeneous; there were no differences in brightness across any crystal examined.

Microscopic Homogeneity. The *microscopic* homogeneity of the Co_xNi_{1-x}(pc)I was determined by examining the EPR spectra of the deiodinated samples Δ-Co_xNi_{1-x}(pc), because deiodinated materials are insulators and their magnetic properties are not complicated by the presence of mobile charge carriers. Thus, as x becomes small, resolved ^{59}Co ($I = {}^7/_2$) hyperfine structure is expected if the Co(pc) is microscopically dispersed in the diamagnetic Ni(pc), whereas a reduction in signal strength without a shape change would signal extensive segregation. The deiodination procedure was conducted in vacuo (10^{-3} Torr) at a temperature of ~100 °C, substantially below the sublimation point of metallophthalocyanines ($T_{sub} \sim 400$ °C, 10^{-3} Torr). Thus, molecular migration will not occur during this procedure and the

(4) (a) Schramm, C. J.; Scaringe, R. P.; Stojakovic, D. R.; Hoffman, B. M.; Ibers, J. A.; Marks, T. J. *J. Am. Chem. Soc.* **1980**, *102*, 6702–6713. (b) Martinsen, J.; Greene, R. L.; Palmer, S. M.; Hoffman, B. M. *J. Am. Chem. Soc.* **1983**, *105*, 677–678. (c) Martinsen, J.; Tanaka, J.; Greene, R. L.; Hoffman, B. M. *Phys. Rev. B: Condens. Matter* **1984**, *30*, 6269–6276.

(5) For an analogous study of alloys of organic conductors, see: Miller, J. S.; Epstein, A. J. *Angew. Chem., Int. Ed. Engl.* **1987**, *26*, 287–293.

(6) Oertling, W. A.; Salehi, A.; Chung, Y. C.; Leroi, G. E.; Chang, C. K.; Babcock, G. T. *J. Phys. Chem.* **1987**, *91*, 5887–5898.

(7) (a) Phillips, T. E.; Anderson, J. R.; Schramm, C. J.; Hoffman, B. M. *Rev. Sci. Instrum.* **1979**, *50*, 263–265. (b) Chaikin, P. M.; Kwak, J. F. *Rev. Sci. Instrum.* **1975**, *46*, 219–220.

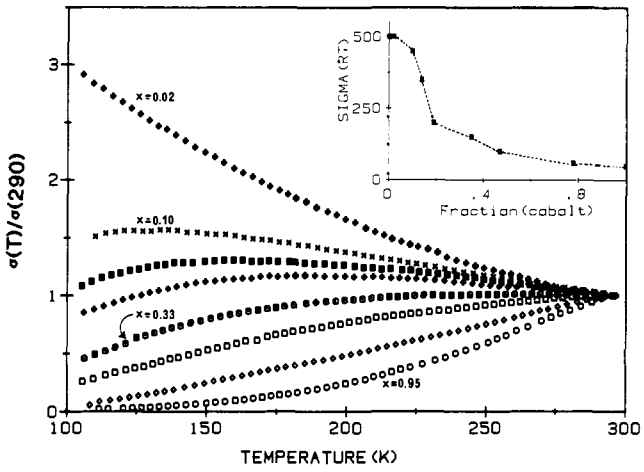

Figure 2. Relative conductivity ($\sigma(T)/\sigma(290\,K)$ of alloys, Co_xNi_{1-x}(pc)I, x = 0.02, 0.10, 0.15, 0.20, 0.33, 0.50, 0.75, and 0.95. Within the variability of samples, x = 0 (Ni(pc)I) and x = 0.02 are indistinguishable, as are x = 1 (Co(pc)I) and x = 0.95. Inset: Room-temperature conductivity (Ω^{-1} cm^{-1}) vs fraction of Co(pc) units, x. The dotted line is to guide the eye. These results are averages of measurements on numerous crystals. For a given material, uncertainties in crystal measurements lead to errors in σ(RT) of ca. ±15%.

distribution of the component molecule in the deiodinated samples will reflect that for the conductive materials.

In pure Co(pc) the interplay between dipolar broadening of the Co^{2+}-ion signal and exchange interactions among the spins leads to a simple spectrum with axial symmetry without resolved hyperfine structure (Figure 2). Mixtures of Co(pc) and Ni(pc) prepared by grinding exhibit the spectrum of pure Co(pc), but with the intensity proportional to the fraction of Co(pc). However, deiodinated samples with $x < 1$ show Co^{2+} hyperfine structure that becomes increasingly well defined as x is decreased (Figure 1) and that clearly arises from isolated Co(pc) at low x.[8] These results indicate that the dipole–dipole and exchange interactions between Co^{2+}(pc) spins progressively decrease as x decreases. They show that the Co(pc) in the Δ-Co_xNi_{1-x}(pc) and thus in the oxidized materials are dispersed with the Ni(pc), and therefore the Co_xNi_{1-x}(pc)I may be viewed as solid solutions or alloys of the parent molecular conductors. A related study of alloys Cu_xNi_{1-x}(pc)I between Cu(pc)I and Ni(pc)I reached the analogous conclusion.[9]

Properties of Co_xNi_{1-x}(pc)I. Single-Crystal Conductivity. Room-temperature four-probe conductivities (σ_{RT}) of the alloys, Co_xNi_{1-x}(pc)I decrease from that of Ni(pc)I (x = 0) to that of Co(pc)I (x = 1) as x increases (Table II), as depicted in the inset of Figure 2. The major change in σ_{RT} occurs as x is increased to 0.25. The main figure plots the normalized conductivity of each alloy in the temperature range from ambient temperature to 100 K. As x is increased, the conductivity smoothly changes from the metallike behavior of the x = 0 compound, Ni(pc)I[3] ($d\sigma/dT < 0$), to the unusual, roughly linear dependence on temperature of Co(pc)I[4] (x = 1). Again, the major change occurs at low values of x. The temperature response of the conductivity of very dilute Co_xNi_{1-x}(pc)I, x = 0.02, is nearly like that of Ni(pc)I, but alloys of x = 0.10, 0.15, 0.20, and 0.33 already exhibit smooth reproducible conductivity maxima over the temperature range 170–260 K. The temperature of the maximum increases with the amount of Co(pc)I, and for $x < 0.33$ the conductivity decreases smoothly as the sample is cooled below ambient.

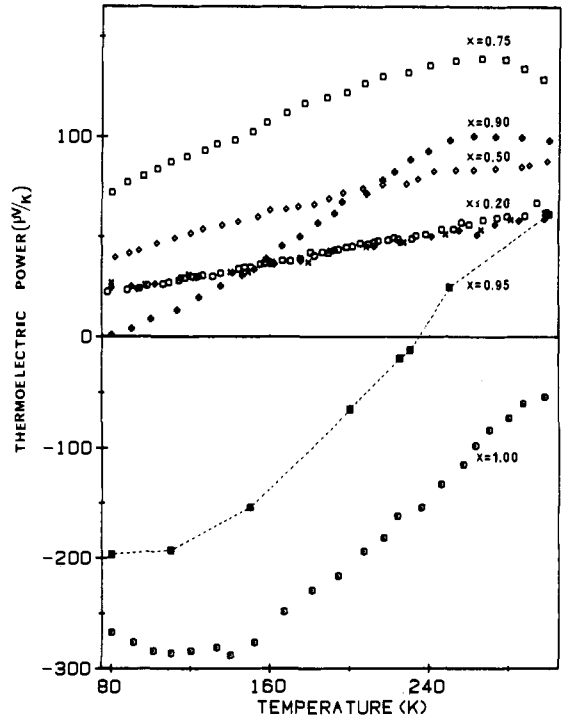

Figure 3. Thermoelectric power (μV K^{-1}) of alloys, Co_xNi_{1-x}(pc)I, x = 0.02, 0.10, 0.20, 0.50, 0.75, 0.90, 0.95, and 1.00.

Thermoelectric Power. Thermoelectric power data for temperatures between 80 and 300 K are shown in Figure 3 for a large number of alloy compositions. For $x \leq 0.20$, the results are similar to data for the pure Ni(pc)I[4] (x = 0); as predicted for a quasi-1-D metal where the carriers are holes on the macrocycle, the thermopower is relatively small and positive and increases linearly with temperature. For x = 1 we earlier reported that S is large and negative, with a value that increases with decreasing temperature as seen for a semiconductor; this was interpreted as indicating that the carriers are electrons in a one-third-filled band on the metal spine. Surprisingly, as x is raised above 0.2 the $S(T)$ curves do not smoothly vary between the limiting x = 0 and x = 1 curves, as occurs for the conductivity. Instead, as x is increased above 0.2, S first becomes significantly more positive, with the largest values being reached for x = 0.75. Only with x = 0.90 and 0.95 is there a precipitous change toward the x = 1 curve.

In a partially filled tight-binding band, the thermopower (neglecting correlation effects) may be written[10]

$$S = \frac{2\pi^2}{3}\frac{k_B}{e}\frac{k_BT}{4t}\left\{\frac{\cos(\pi\rho/2)}{\sin^2(\pi\rho/2)} + 2t\frac{\tau'(\epsilon)}{\tau(\epsilon)}\bigg|_{E_F}\right\} \quad (1)$$

where ρ is the number of electrons per site ($0 \leq \rho \leq 2$), $4t$ is the bandwidth. ϵ is the single particle energy, τ is the single-particle scattering time, and τ' is the energy derivative of τ. For oxidation of $^1/_3$ electron/M(pc) as occurs here, if the site of oxidation is the doubly filled HOMO of the macrocycle, then $\rho = 2 \times {}^5/_6$; if the site is the singly occupied d_{z^2} orbital of the cobaltous ion, $\rho = 2 \times {}^1/_3$. For normal scattering mechanisms, the two terms in brackets are temperature independent to first order and of about equal size. Thus for fixed ρ, S should be proportional to T. This is seen for Ni(pc)I, where the carriers are holes associated with π-orbitals of the macrocycle and $\rho = {}^5/_3$,[4] as well as for alloys with $x \leq 0.2$ (Figure 3).

Thus we may with reasonable certainty conclude that within the composition range $0 \lesssim x \lesssim 0.2$ the π-band filling of $\rho = {}^5/_3$ as well as τ/τ' remains constant. The unchanging filling of the

(8) (a) Ignoring a slight rhombic splitting in the spectrum, the EPR spectra of Δ-$Co_{0.1}Ni_{0.9}$(pc) In Figure 2 yield spin Hamiltonian parameters of $A_\parallel$ = 0.017 and $A_\perp$ = 0.032 cm^{-1}, $g_\parallel$ = 2.0 and $g_\perp$ = 3.2. These values are comparable to the literature values, $g\parallel$ = 1.89, $g_\perp$ = 2.94, $A_\parallel$ = 0.015, and $A_\perp$ = 0.028 cm^{-1}, which were obtained from the magnetically diluted Co(pc) In Ni(pc) ($^1/_{1000}$) at 77 K and 27 K.[8b,c] (b) Assour, J. M.; Kahn, W. K. *J. Am. Chem. Soc.* **1965**, *87*, 207–212. (c) Manoharan, P. T.; Rogers, M. T. *Electron Spin Resonance of Metal Complexes*; Yen, T. F., Ed.; Plenum Press: New York, 1969; pp 143–173.

(9) Liou, K. K.; Ogawa, M. Y.; Palmer, S. M.; Quirion, G.; Poirier, M.; Hoffman, B. M. *Phys. Rev. B*, in press.

(10) Chaikin, P. M.; Greene, R. L.; Etemad, S.; Engler, E. *Phys. Rev. B* **1976**, *13*, 1627–1632.

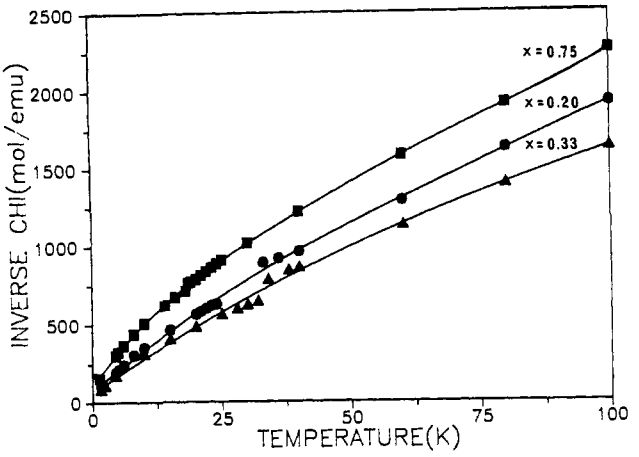

Figure 4. Inverse bulk magnetic susceptibility (emu mol^{-1}) of Co_xNi_{1-x}(pc)I plotted as a function of temperature (kelvin), for $x = 0.20$, 0.33, and 0.75. The solid lines are the best fit of the data to eq 3.

macrocycle π-band means that in this concentration range Co enters as $Co^{2+}(d^7)$ with a localized spin. The decrease in conductivity as x is increased (Figure 2) implies that τ itself decreases rapidly with x; the decrease in conductivity presumably arises from increasing magnetic scattering from the Co^{2+} spins as we have seen in partially oxidized Cu^{2+} macrocycles,[9,11] eventually leading to low-temperature localization of the carriers.

As x is increased to $x = 0.50$ and 0.75, S increases rapidly. It is straightforward to interpret this as a consequence of a decreased partial oxidation of the macrocycle and a gradual filling of the ligand–π-band (ρ shifts from $^5/_3$ toward 2), which causes S to increase according to eq 1. It follows that nonstoichiometric oxidation of Co^{2+} ions must begin to occur in this concentration range, although the conductivity and thermopower still remain dominated by carriers in the π-band of the macrocycle. Assuming the ρ-dependence of eq 1 and starting with $\rho = 1.667$ for $x = 0$, we infer $\rho = 1.72$ for $x = 0.50$ and $\rho = 1.77$ for $x = 0.75$. The temperature response of S at $x = 0.75$ is more easily understood as resulting from a temperature dependence of ρ, with the "hole" shifting increasingly to the metal site as T decreases. For $x = 0.95$, the crossover to metal-spine conduction is observed. If we assume that there are two parallel but independent conduction channels, the π-band (σ_π,S_π) and the metal spine (σ_M,S_M), the measured thermopower is given by[12]

$$S = \frac{\sigma_\pi}{\sigma_\pi + \sigma_M} S_\pi + \frac{\sigma_M}{\sigma_\pi + \sigma_M} S_M \qquad (2)$$

From this equation, we infer that $\sigma_M > \sigma_\pi$ only for $x \leq 0.95$. Without independent knowledge of $\rho(x)$, it is not possible to make a detailed separation of the transport parameters. However, the above interpretation agrees qualitatively with the magnetic data presented below, in particular the x dependence of the Curie constant.

Magnetic Susceptibility Measurements. The static magnetic susceptibilities of Co_xNi_{1-x}(pc)I with $x = 0.15$, 0.20, 0.33, and 0.75 were measured for temperatures 2–300 K. Figure 4 presents plots of χ^{-1} versus temperature; the data for $x = 0.15$ sample are omitted for clarity. These susceptibilities can be fit to eq 3, which

$$\chi(T) = C_{obs}/(T - \theta) + \chi_p \qquad (3)$$

represents the sum of Curie–Weiss contribution from the Co^{2+} local spins and a Pauli term caused by carrier spins;[12] the fitting parameters are given in Table II. The temperature-independent term was found to be approximately the same for all the alloys, $\chi_p \sim 2 \times 10^{-4}$ emu mol^{-1}, similar to those of other M(pc)I.

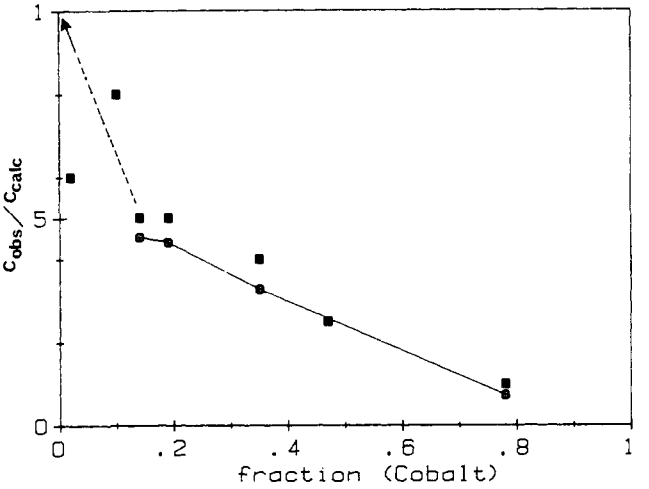

Figure 5. Ratios C_{obs}/C_{calc} (○) and I_{alloy}/I_{bulk} (■) (I = intensity of the EPR resonance; bulk = physical mixture of KBr and Co(pc)) vs fraction of Co(pc) units in alloy and bulk, x.

Up to composition $x \sim 0.33$, the Curie constant increases with x, although not proportionately; it then decreases with further increase in x, vanishing for Co(pc)I ($x = 1$). This behavior of the cobalt local moments is best displayed in a plot of the composition dependence of the relative susceptibility at 77 K, which corresponds to the ratio (C_{obs}/C_{calc}), versus composition (Figure 5). Here C_{calc} is that calculated by assuming one cobalt(II) spin per Co(pc) site:[13]

$$C_{calc(x)} = xS(S + 1)g^2\beta^2/3k_B \qquad (4)$$

$S = {}^1/_2$ and the average of the Co^{2+} g value squared is calculated by eq 5, using $g_\parallel = 2.0$ and $g_\perp = 3.2$ taken from the EPR spectra

$$g^2 = (g_\parallel{}^2 + 2g_\perp{}^2)/3 \qquad (5)$$

of deiodinated alloys. This plot shows that the ratio approaches only unity as $x \rightarrow 0$ (dilute alloy) and that it decreases as the concentration of Co(pc) is increased. The data for $x \rightarrow 0$ support the inference drawn above that in dilute alloys the cobalt sites largely retain the Co^{2+} valence and concomitant $S = {}^1/_2$ local moment; results at higher x clearly indicate that the site of oxidation shifts to the metal ion and/or that antiferromagnetic exchange coupling is introduced.

EPR Spectra of Oxidized Samples. EPR studies of the pure oxidized materials, Co(pc)I ($x = 1$) and Ni(pc)I ($x = 0$), found that the latter shows a free-radical-like EPR signal from carriers associated with the aromatic macrocycles, whereas the former has no resonance except for a weak impurity peak. The room temperature EPR spectra of alloys, with $x \lesssim 0.3$ show broad resonances typical of a metal-ion site but with g values shifted toward $g \sim 2$. This is consistent with the presence of Co local moments that are exchange coupled to the π-carriers, in which case the g value would be the susceptibility-weighted average and in a dilute alloy would be strongly shifted from that of the isolated Co(pc) signal:

$$g = f_{Co}g^{Co} + f_\pi g^\pi \qquad (6)$$

where f_{Co} and f_π are the fractional contributions of the first and second terms of eq 3, and this equation is an analogue to eq 2. The intensities of these broad peaks follow the same trend as the observed values of the Curie constants, with alloys $x > 0.33$ having resonances that are too weak and broad to be detected even at high gain.

Upon cooling the samples, the EPR lines narrow strongly and the signals are easily detectable over a wide range of x; the change in the signal observed for $x = 0.15$ upon lowering the temperature from ~300 to 77 K is shown in Figure 6. The peak profiles of

(11) (a) Quirion, G.; Ogawa, M. Y.; Hoffman, B. M.; Poirier, M. *Solid State Commun.* **1987**, *64*, 613–616. (b) Quirion, G.; Liou, K. K.; Ogawa, M. Y.; Hoffman, B. M.; Poirier, M. *Phys. Rev. B* **1988**, *37*, 4272–4275.

(12) See, for example: MacDonald, D. K. C. *Thermoelectricity: An Introduction to the Principles*; Wiley: New York, 1962.

(13) Carlin, R. L.; Van Duyneveldt, A. J. *Magnetic Properties of Transition Metal Compounds*; Springer: Berlin, 1920.

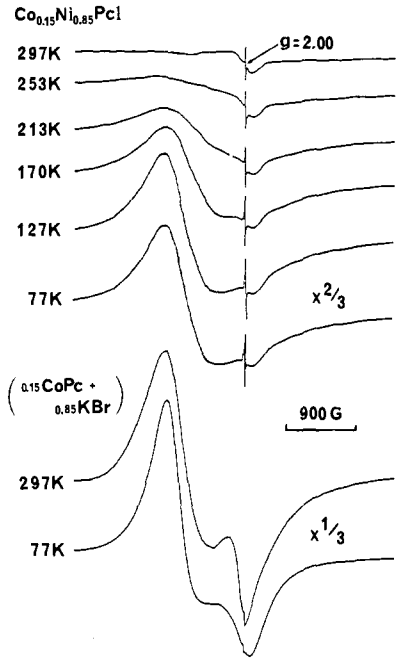

Figure 6. Variable-temperature EPR spectra of $Co_{0.15}Ni_{0.85}(pc)I$ and spectra of the mixture 0.15 Co(pc) + 0.85 KBr (by weight) taken at X-band (9.15 GHz).

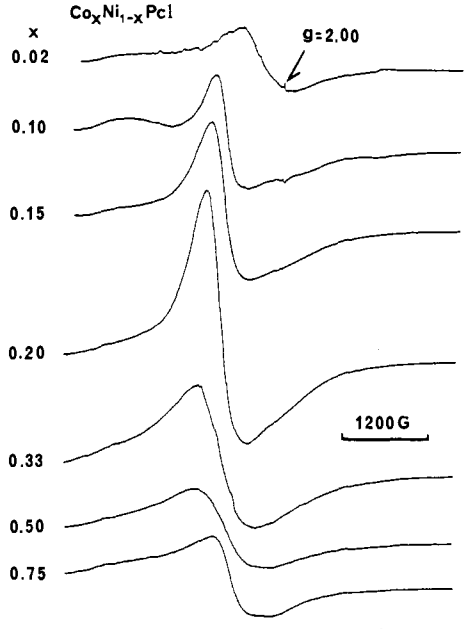

Figure 7. The 77 K EPR spectra of $Co_xNi_{1-x}(pc)I$ for x = 0.02, 0.10, 0.15, 0.20, 0.33, 0.50, and 0.75 (the x = 1 material gives no signal taken at X-band; 9.15 GHz).

these alloys remain the same upon further cooling from 77 to 5 K. At 77 K, EPR spectra of various alloys were recorded under identical experimental conditions, with the same amount of sample (~15 mg). The signal becomes stronger, although not proportionately, as the percentage of Co(pc) increases to x = 0.33 then decreases as expected from the reduced Curie constant with further increase of x (Figure 7). In all of the iodinated conducting alloys, even for low x, Co^{2+} hyperfine structure is absent, in contrast to the nonconducting, deiodinated samples (Figure 1). This absence is interpreted to arise from magnetic exchange and/or dynamic interchange between the Co^{2+} spins and itinerant carriers. The ratio of the EPR intensities of the alloy spectra to those of macroscopically mixed samples of Co(pc) and diamagnetic KBr at 77 K also is plotted in Figure 5. Above the composition x = 0.15 the relative susceptibility and relative EPR intensity are well matched, decreasing roughly linearly with x: scatter at lower

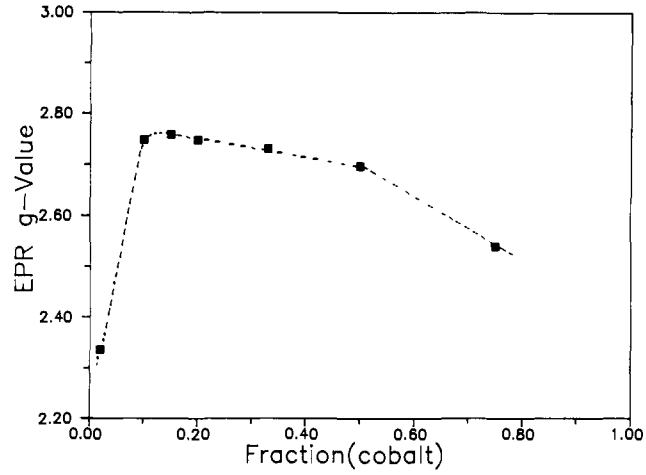

Figure 8. Composition (x) dependence of the $g_\perp$ value of $Co_xNi_{1-x}(pc)I$ at 77 K. The dotted line is to guide the eye.

compositions probably is caused by low EPR intensities, which makes quantitation difficult. The results show that in the alloys with $x \rightarrow 0$ Co(pc) is first incorporated into Ni(pc)I as a ring-oxidized impurity bearing a Co^{2+} ($S = {}^1/_2$) localized moment.

For the alloy with the lowest amount of Co(pc), x = 0.02, the g value at 77 K is much smaller ($g_\perp$ = 2.34) than that of the unoxidized material ($g_\perp$ = 3.2), demonstrating that there is a coupling between the local Co^{2+} spins and the carrier spins that leads to a single signal with a susceptibility-weighted g value as described by eq 6. Consistent with this picture, upon increase of the percentage of Co(pc), the g value first increases strongly (x = 0.02, $g_\perp$ = 2.34; x = 0.10, $g_\perp$ = 2.75). The slow decrease of g upon further doping of Co(pc) into Ni(pc) ($x \geq 0.20$; Figure 8) we take to reflect the fact that there is partial oxidation both from macrocycle π-orbitals and cobalt d_{z^2} orbitals of the metal spine, with dynamic interchange between sites averaging the g values. Thus, the charge-transport and EPR measurements both support a picture of a two-band conductivity for intermediate compositions. Such a picture also is supported by preliminary XANES measurements.[14]

Summary

The alloys of the molecular conductors Co(pc)I and Ni(pc)I have been prepared and proven to be homogeneous by microprobe analysis and by EPR measurements on deiodinated samples. As the percentage of Co(pc)I is increased from x = 0 in the alloys, $Co_xNi_{1-x}(pc)I$, there is a smooth change from the highly conducting metallic behavior of Ni(pc)I to the nonmetallic behavior of Co(pc)I (x = 1). In dilute alloys with $x < 0.2$, the cobalt ion sites retain their Co^{2+} valency, and the associated $S = {}^1/_2$ local moments act as paramagnetic scattering centers for the macrocycle-based hole carriers produced by partial oxidation of the pc ring. As x is increased beyond ~0.2 there is a progressive shift to the metal-ion spine as the site of oxidation. For these intermediate values of x charge transport involves both the metal spine and the macrocycle with charge interchange between them that is composition and temperature dependent; however, the better conductivity of the hole carriers on the latter causes them to dominate the thermopower which becomes increasingly positive until $x \gtrsim 0.75$. Only by $x \sim 0.95$ and at $T \sim 240$ K does the thermopower become negative, which can be taken as the crossover point at which all transport properties are determined by the carriers associated with the metal spine as in the limiting case of Co(pc)I (x = 1).

Acknowledgment. This work has been supported by the Solid State Chemistry Program of the National Science Foundation (Grant DMR-8818599, B.M.H.) and by the Northwestern University Materials Research Center under the NSF-MRL program (DMR-8821571, B.M.H.).

(14) Scott, R.; Eidsness, M.; Liou, K. K.; Hoffman, B. M., to be published.